

Technology Development and Testing for Enhanced Mars Rover Sample Return Operations[†]

Richard Volpe
Mailstop 198-219
818-354-6328

Eric Baumgartner
Mailstop 82-105
818-354-4831

Paul Schenker
Mailstop 125-224
818-354-2681

Samad Hayati
Mailstop 180-603
818-354-8273

Jet Propulsion Laboratory
California Institute of Technology
Pasadena, California 91109
Email: *firstname.lastname@jpl.nasa.gov*

Abstract—This paper describes several Jet Propulsion Laboratory research efforts being conducted to support Mars sample return in the coming decade. After describing the 2003/05 mission scenario, we provide an overview of new technologies emerging from three complementary research efforts: Long Range Science Rover, Sample Return Rover, and FIDO Rover. The results show improvements in planning, navigation, estimation, sensing, and operations for small rovers operating in Mars-like environments.

TABLE OF CONTENTS

1. INTRODUCTION
2. MARS SAMPLE RETURN MISSION SCENARIO
3. LONG RANGE SCIENCE ROVER TECHNOLOGIES
4. SAMPLE RETURN ROVER TECHNOLOGIES
5. FIDO ROVER TECHNOLOGIES
6. SUMMARY
7. ACKNOWLEDGMENTS

1. INTRODUCTION

Even before Sojourner made its first wheel tracks on Mars in 1997, it was anticipated that this rover would be only the first in a series of surface exploration spacecraft targeted for the planet. While it will be Sojourner's flight spare that drives on Mars in 2002, the next leap in technical capability exhibited by rovers will be in the 2003/05 mission set, where much larger rovers will perform rock and soil sample collection for return to Earth. These rovers will have greater innate capabilities, opening the door for the insertion of new robotics technologies that have been in development since the inception of the Pathfinder mission five years ago. Among these are on-board stereo vision processing, autonomous landerless operations, manipulation and instrument positioning by arms, precision navigation for rover/lander rendezvous, and distributed ground operations.

Of fundamental importance to the incorporation of the new capabilities on next-generation rovers is the use of a more capable electronics, sensing, and instrumentation infrastructure located on-board the rover. For instance, as Sojourner was being prepared for flight, JPL was constructing a new prototype, Rocky 7 [16]. Several key features were added to support long trips away from the lander: a deployable mast to

raise cameras and take panoramic images of the surrounding terrain, a shorter arm for sample acquisition and instrument placement, and a sun sensor to accurately determine heading while driving. These features were demonstrated during field tests in the Mojave Desert in 1997, which led directly to the acceptance of the 03/05 missions [15].

The selected 03/05 mission concept, however, requires an enlarged rover that has the added functionality of carrying a drill for rock sampling, larger wheels for enhanced mobility, and a significantly upgraded science instrument suite (as opposed to the Sojourner rover). Therefore, to support continued field tests with the selected science team for the 03/05 mission, a new Field Integrated Design and Operations (FIDO) rover was conceived, designed, integrated during a 12-month period, and demonstrated in desert tests in April 1999 [14]. The FIDO rover reflects the current engineering sensors and science instrument suite that are planned for the 03/05 mission. While this rover will continue to act as an operations testbed for mission scientists, it has a second function as an integration testbed for new technologies that continue to be developed by ongoing research efforts.

The JPL core robotics technology program has been supporting these research efforts, which include the Rocky 7 rover as well as another platform, the Sample Return Rover (SRR) [13]. Each rover has been dedicated to increasing autonomy in two respective halves of the exploration problem: autonomous motion away from and back to the lander. New techniques used include estimation and visual localization, on-board path and sequence re-planning, and natural and man-made target recognition and tracking.

This paper describes these techniques, as well as the details of the mission scenario in which they will be used. Section 2 describes the Mars Sample Return's Athena rover mission. The technology developments associated with the Long Range Science rover task are discussed in Section 3, while the Sample Return Rover and the development of rendezvous techniques are described in Section 4. The Athena terrestrial prototype rover, FIDO, is discussed in Section 5, and summary remarks are provided in Section 6.

[†] 0-7803-5846-5/00/\$10.00 © 2000 IEEE

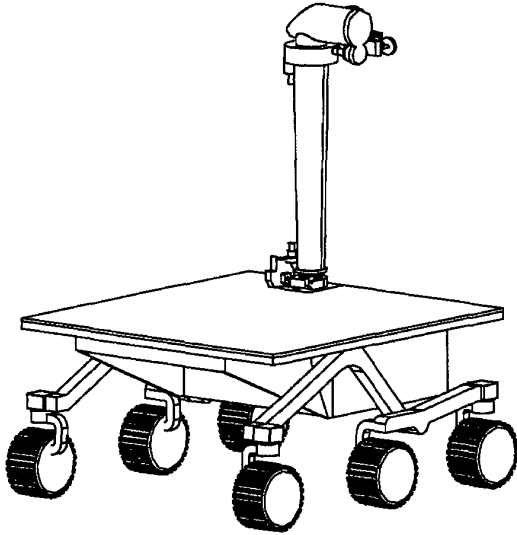


Figure 1. Preliminary drawing of the Mars Sample Return Athena-Rover.

2. MARS SAMPLE RETURN MISSION SCENARIO

Launching in 2003 and again in 2005, NASA's Mars Sample Return (MSR) spacecraft will place two science rovers on the surface of the planet. These rovers will be carried to the surface on the top deck of a three-legged lander that is roughly 1 m tall and 3 m in diameter. This size, substantially larger than previous landers of the 1996, 1998, and 2001 missions, makes it possible to carry a sample-return Mars Ascent Vehicle (MAV) as part of the lander payload. The lander size also enables the use of a rover that is approximately twice the size of the Pathfinder mission rover, Sojourner, in every dimension. (Sojourner was 60 x 40 x 35 cm.) A preliminary drawing of this "Athena-class" rover is shown in Figure 1.

The larger size of this MSR rover is needed to support rock sampling operations and to carry the seven science instruments that make up its payload. Rock sampling is accomplished using a coring drill, which relies on the rover mass to provide the force behind it in its vertical operating configuration. The science instruments are used to select the target rocks for sampling, to determine the composition of the rock samples obtained, and to study rocks in the surrounding area. Four of the instruments, located on a five degrees-of-freedom arm, require close proximity to the sample to be measured. Two others, located on a 1 m mast, require only line of sight to the target. The drill, itself, is the seventh instrument.

The rover will begin its mission on the lander top deck by obtaining a panorama of the surrounding terrain for science, engineering, and public outreach purposes. From these images, a ramp deployment direction will be selected, as well as initial travel routes and goals for the first rover traverse. After ramp deployment, the rover will drive to the surface and begin navigating the terrain. The maximum distance driven each day will be 100 m, and often much less, especially when the rover is positioning itself for science operations.

During the mission, communication with the rover will nominally take place twice per day, relayed by the lander. Each communication window will allow a limited set of images and data to be transmitted to operators on earth, while new instructions are provided to the rover based on the previous communication cycle. Typically the rover will receive instructions for the day in the morning, and transmit the results and status at the end of the day.

After obtaining its first set of rock samples, the rover will return to the lander and deposit them in the MAV. This must be accomplished by successfully aligning with the base of the ramp, driving up its two narrow rails, and accurately detecting the proper position for sample transfer. At this location, the MAV payload door will be opened and the sample transfer will be completed robustly and autonomously; thermal considerations require that the payload door be open less than that of the typical communications cycle.

Since mission constraints limit surface operations to less than 90 days, the sample acquisition and return to MAV cycle can be performed only three times at most. It is likely, however, that each cycle will see the rover venturing farther from the lander.

After the last sample return operation, the rover will move off the lander deck and far enough away from the lander to prevent its being damaged during the MAV lift-off. This launch is expected to damage the lander communication system and prevent it from acting as a relay for the rover. Therefore, the rover will use auxiliary communication to an orbiter, to enable it to perform the extended mission of exploring the surface.

Obviously, the complexity and accuracy of the autonomous operations described above directly influence the amount of science operations that will be performed. For this reason, JPL research projects aim to introduce new functionality and features into Mars rovers to enable greater science return from all upcoming Mars rover missions. Techniques for more autonomous and robust exploration and return to the lander have been developed and implemented in field tests. Each of these efforts is described next.

3. LONG RANGE SCIENCE ROVER TECHNOLOGIES

To improve rover navigation, exploration, and autonomy, the Long Range Science Rover (LRSR) research task has been improving the rover's ability to navigate through the environments, while maintaining an accurate sense of its position. This section describes advances in four pertinent areas: dynamic sequence generation, autonomous path planning, visual localization, and state estimation. All research was conducted with the prototype rover, Rocky 7, shown in Figure 2.

Dynamic Sequence Planning

On-board planning with dynamic sequence generation allows ground controllers to provide much higher level commands, while increasing the optimality and robustness of rover opera-

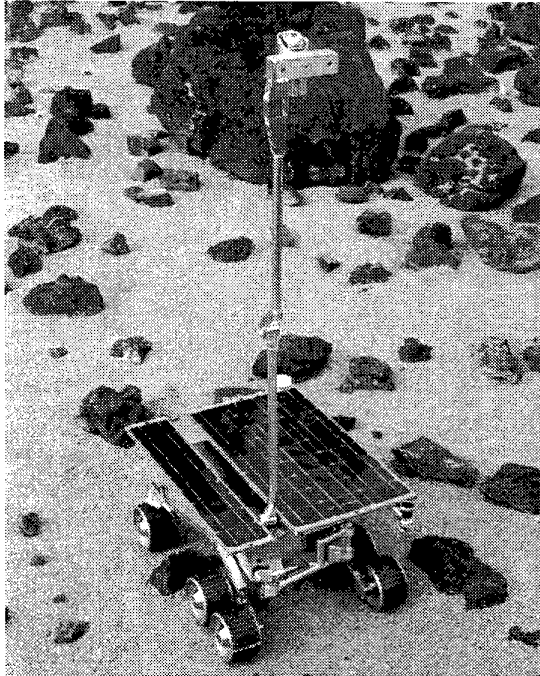


Figure 2. The Rocky 7 research prototype.

tions on the surface. For instance, during the Pathfinder Mission, the Sojourner rover [10] was provided with extremely detailed sequences daily, fatiguing operators while also disallowing contingency operations when the flow of execution was non-nominal. Contrary to this, we have been experimenting with on-board replanning that can change the execution of daily activities based on unanticipated variations in quantities such as position, terrain, power, and time. To accomplish this, we have used a dynamic on-board planning system called CASPER (Continuous Activity Scheduling, Planning, Execution, and Replanning) [5], [6].

Figure 3 shows an example scenario in map form, where dark orange shapes represent obstacles known a priori (e.g. from lander descent imagery). In this case, the initial plan for the traverse will bring the rover to an unexpected obstacle near the first goal, represented as a light orange shaded shape. Circumnavigation around this obstacle will move the rover closer to other goals, triggering CASPER to recognize the situation and re-plan to visit the closest goal first. We are currently evaluating this and similar scenarios experimentally.

Autonomous Path Planning

For the longer traverses required of upcoming missions, autonomous path planning is desirable since operators will not be able to see three-dimensional terrain features out to the more distant goal locations. Whereas Sojourner drove a total of 84 m during its entire mission, the MSR Athena rover will be capable of driving this distance in a single day. However, stereo imagery of the terrain provided to operators will only have an envelope of 20 m at best resolution. Therefore, the path planning advances described here will allow the rover to be its own operator. It can image the terrain from periscopic

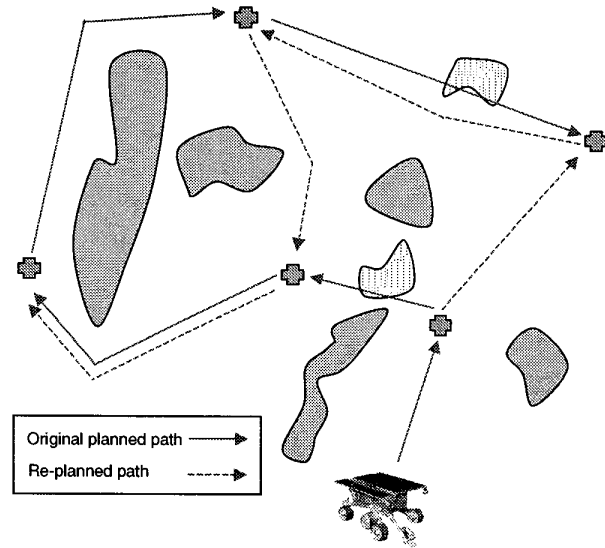


Figure 3. After encountering a previously unknown obstacle shown in light orange, CASPER replans the sequence of targets. Blue crosses are the goal locations, and dark orange shapes are obstacles known a priori.

cameras, select a path through the terrain to the edge of the effective stereo range, and repeat the process until the goal is achieved. A representative example of a partial panorama and the resulting elevation map of the terrain are shown in Figure 4.

Rocky 7 uses a local sensor-based path planner called *Rover-Bug* [8], [9]. This algorithm was developed for vehicles that have limits on sensor range, field of view, and processing. The two main modes of operation are *motion-to-goal* and *boundary-following*, which are used to provide global convergence.

Rover-Bug works by using the local elevation map to construct a map of convex hulls around all obstacles in the sensing range. These hulls are then merged and grown to provide a configuration space representation of the sensed terrain. A tangent graph is constructed to determine if there is an unobstructed path to the envelope of the sensed region in the direction of the goal. If one exists, it is followed, and the process is repeated at the end of the path segment to the sensory envelope.

If a free path does not exist, stereo images are obtained to the most promising side of the current view, and the process is repeated. In some cases, the free path places the rover at the edge of the sensory envelope but still obstructed from the goal by an obstacle. In this case, the rover will begin to use its body-mounted cameras to reactively *boundary follow* until there is a clear path to the next goal.

Figure 5 shows experimental data obtained from Rocky 7 while using this algorithm to traverse our MarsYard test area. The start position is in the lower left corner, 21 m from the goal in the upper right. Four sets of sensory data are shown as

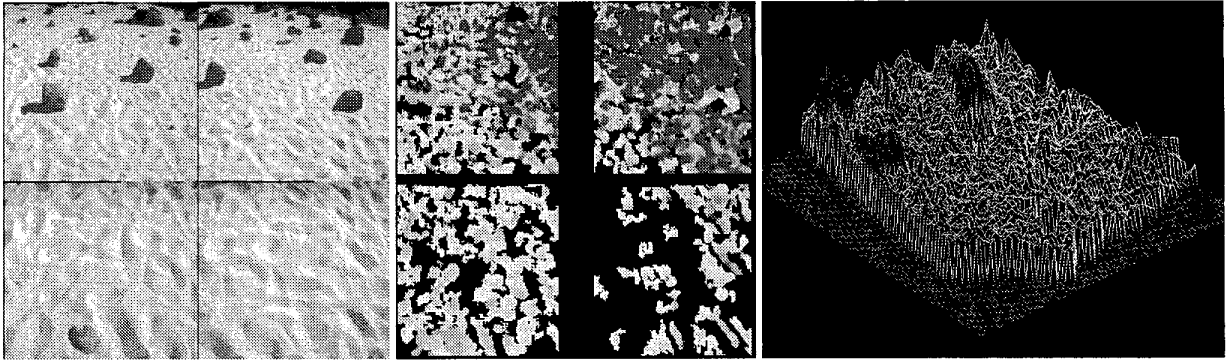


Figure 4. Steps of on-board terrain sensing: panoramic mosaic view from rover mast stereo imager, composite range map extracted from stereo views, and elevation map created from range data.

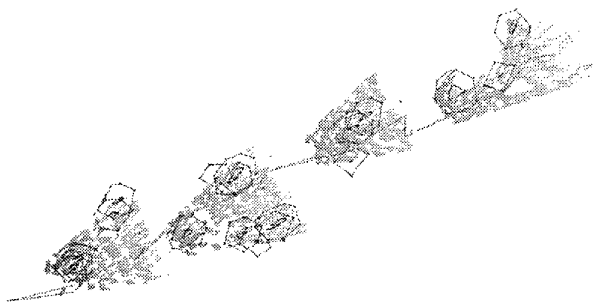


Figure 5. Experimental results from a multi-step run using Rover-Bug in the JPL Mars Yard.

orange wedges along the path. Projected on to these data sets are the pink convex hull representations of the sensed obstacles. The green and blue lines passing through the obstacle field are the planned and executed paths, respectively. The gap between data sets is due to a lack of merging of data from both the mast and body-mounted cameras, and is currently being corrected. The sudden changes in the path direction at the far side of each wedge does not indicated actual rover motion; rather it is an artifact of the estimated rover position that is updated by localization at this point in the traverse. This localization is discussed next.

Visual Localization

Visual localization uses the same terrain imagery as path planning, but for the purpose of monitoring the apparent motion of three-dimensional ground features after the rover has completed a move. In this way, the on-board position estimate of the rover can be updated to compensate for errors caused by wheel slippage or rock bumping. On Pathfinder, this localization functionality was performed manually by operators viewing Sojourner from the fixed position lander cameras, restricting the update to once a day and permitting operations only within the stereo envelope of the lander. In contrast, the terrain-based localization described here has application to many forms of landerless operations: incremental long traverses, local operations within range of a prior stereo panorama, localization in descent imagery, and closed chain rover moves with estimate smoothing.

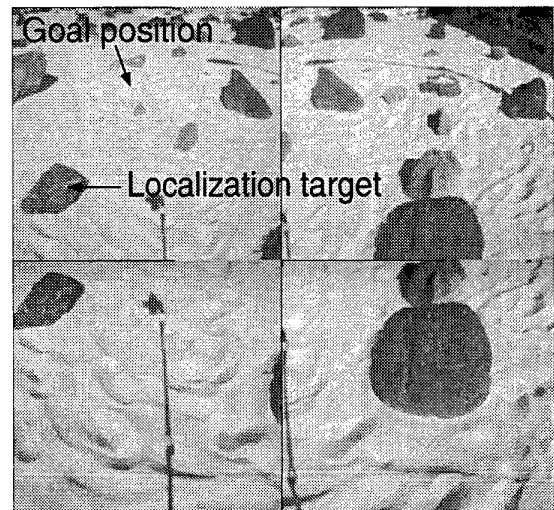


Figure 6. Example of automatic target selection for localization.

The technique relies on obtaining a stereo elevation map from the initial rover position, as shown in Figure 4. This imagery is automatically analyzed based on the range data quality, and the quality expected to be seen at the goal point specified by path planning [11]. Typically, there will be a prominent rock between the two locations. From the analysis, it will be selected as the localization target, and viewed by the rover after reaching the end of the local path segment. Figure 6 shows an example of the automatic target selection, with four images concatenated to provide a reasonable number of potential targets.

To match the two stereo views of the terrain, a multi-resolution search technique is used to provide the best estimate of the displacement of the original elevation map from the final one [12]. Typical results provide position error estimates that are 1% of the distance traveled. However, the search uses the on-board estimate of the rover position as its starting point, so more reliable results are obtained if the initial estimate is more accurate. Therefore, to obtain better continuous position estimates, we have been developing a new estimation technique, discussed next.

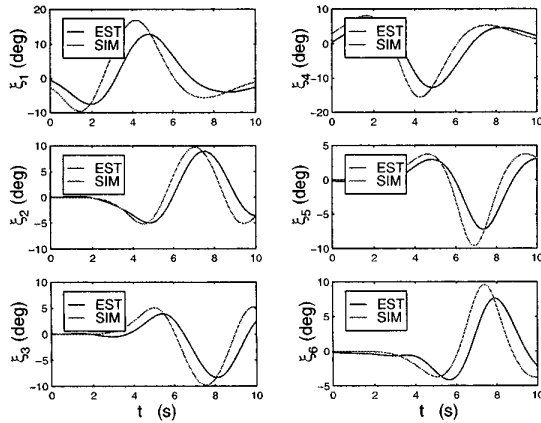


Figure 7. Simulation results showing true values and estimates for wheel contact positions, where the left/right three wheels angles are shown by the left/right side graphs.

Kinematic State Estimation

In addition to periodic visual localization of the rover, we have developed real-time position and heading estimation using all other sensors on the vehicle: angular rate, accelerometer, sun sensor, wheel angle rates, and mobility system linkage (rocker-bogey) configuration. This technique moves far beyond the simple dead reckoning of Sojourner and improves upon our previous advances in position estimation with sun sensing [15]. The results aid navigation during path execution, provide better input to localization, and replace both in visually featureless terrain (e.g., sand dunes) or in the case of visual sensing failure.

The estimator uses a Kalman filter framework, with the process model chosen so that the inertial sensor data are used as an input to drive the process equation. The procedure avoids the difficulty of modeling the detailed process dynamics [1] by exploiting the ability of the Kalman filter to perform the appropriate least-squares averaging of the action of each kinematic chain in the rover. These forward kinematic chains have velocity components defined by the sequence of links joining the rover frame to each estimated wheel contact point, and a component given by the slip between the wheel and the ground. The deterministic component of the slip is used to capture the effects of a known steering action or a known average slip rate over different kinds of terrain.

Both simulation and experimental results with this estimation technique have been conducted. Figure 7 shows the ability of the estimator to correctly track the wheel contact angle over an undulating terrain. The simulation is particularly valuable since ground truth can be known exactly. For instance, using simple integration of the wheel velocity results in a 2% error in measured position, while the estimator reduces the error by an order of magnitude.

Experimental results further support these conclusions. Figure 8 shows the results from Rocky 7 driving over an obstacle on the right side of the vehicle only. While the left side

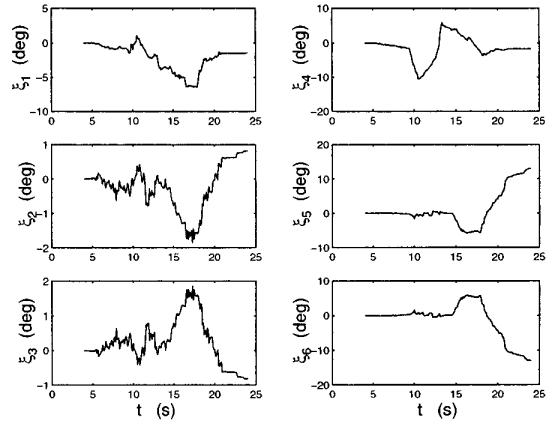


Figure 8. Experimental results from Rocky 7 showing the estimates for wheel contact angles.

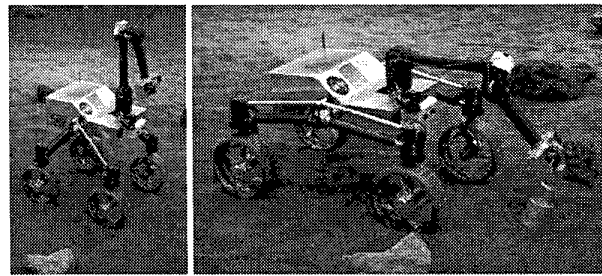


Figure 9. The Sample Return Rover.

wheel contact points change only slightly, the much larger changes in the right side are correctly determined. Note, in the final configuration, the bogey wheels were still on the obstacle, while the steering wheel had completely traversed the obstacle. The estimated wheel contact angles were within 5 degrees of the true values measured independently. Further experiments are in progress, as well as integration of visual position estimation, as described in the next section.

4. SAMPLE RETURN ROVER TECHNOLOGIES

In 1997, JPL began development of the Sample Return Rover (SRR), a small, lightweight rover that investigated focused technology advances in the areas of rover-to-rover and rover-to-lander rendezvous. SRR, shown in Figure 9, is a 7 kg rover with a 4-wheel rocker mobility system that is capable of traversing over obstacles up to 15 cm in height. The rover includes 4-wheel steering and carries a three degrees-of-freedom manipulator arm with a 1 degree-of-freedom gripper. This robot arm is used for panoramic imaging along with sample pick-up and transfer. The rover also includes a posable rocker joint for variable ground clearance and rover reconfiguration in difficult terrain. SRR carries a PC104+ derived electronics system, including a 300 MHz AMD K6 processor, motion control I/O boards (D/A and encoder readers with closed-loop control realized in software), A/D board, PCI color framegrabbers, and a wireless Ethernet.

The original concept for SRR derived from the previous version of the MSR mission where an Athena-class rover tra-

versed long distances, stopped at interesting science sites, and acquired and stored rock and soil samples. During a second mission, a small, lightweight rover would land on the Martian surface and rendezvous with the science rover to retrieve the sample collected during the primary science mission. Such a rover-to-rover rendezvous was demonstrated by the SRR technology team during the summer of 1998 [13]. This rendezvous was accomplished using an RF beacon transmitter and receiver pair for non-line-of-site navigation to the science rover, visual tracking of the static science rover during line-of-sight navigation, determination of rover-to-rover pose using man-made features located on the science rover, and, terminal guidance to the sample cache container and pickup of this container using the on-board manipulator arm.

In 1999, the SRR task turned its attention to the rover-to-lander rendezvous problem in support of the MSR mission and the requirement that the Athena rover return its cached samples to the lander and the awaiting MAV, as described in Section 2. Some of the technology developments established during the rover-to-rover rendezvous application were transferred to the rover-to-lander rendezvous problem. The requirements of the Athena rover mission, however, necessitated the development of new techniques for the robust and accurate navigation of SRR with respect to the lander such that autonomous lander acquisition, lander rendezvous, and ramp climbing are possible with minimal, if any, ground support. Figure 10 depicts the scenario associated with the rover-to-lander rendezvous problem in terms of the multi-phase operations and technologies used during the return to the lander. The rover-to-lander rendezvous problem is divided into the following phases:

- Long distance visual tracking using lander texture features derived in the wavelet space
- Multi-point tracking of lander features for heading and range estimation of the rover relative to the lander
- Ramp location determination using lander features
- Ramp recognition using cooperative ramp features for heading and range estimation of the rover relative to the bottom of the ramps

The long-distance navigation of SRR relative to the lander is accomplished with a novel wavelet-based detection algorithm for the long-range visual acquisition of a lander from greater than 100 m using a single, black-and-white rover imaging system (20 degree field of view) [4]. This information enables autonomous correction the rover heading with respect to the lander, and to guidance of SRR to within 25 m of the lander. Such a navigation sequence is shown in Figure 11. Within 25 meters of the lander, a visual technique that takes advantage of the known geometry of the lander structure is used to track multiple features (e.g., lander leg struts, lander deck, etc.) to determine the pose of the rover relative to the lander. Preliminary results indicate that precision on the order of 50 cm in range and 1 to 2 degrees in orientation is possible using this approach.

Likewise, the known ramp geometry allows for the visual acquisition of the lander ramps and the relative positioning of the rover relative to the ramps. These techniques combine to produce a navigation strategy for the autonomous guidance

of the rover from 25 m from the lander to 5 m in front of the ramps. Finally, visual acquisition of the lander ramps is accomplished using cooperative markings from which rover-to-ramp position and heading information is obtained. The successive visual acquisition of the lander ramps brings the rover from 5 meters to within 5 cm of the bottom of the lander ramps. Many successful experiments have been accomplished in both laboratory and outdoor settings. These results indicate that the rover can reliably and robustly navigate to the bottom of the ramps with an absolute precision of 1 cm in lateral and longitudinal offset and less than 1 degree orientation error with respect to the ramps. As such, the combination of these rover navigation techniques leads to a single-command autonomous sequence associated with the return to the lander and the regress of the rover up the lander ramps to deposit the sample cache in the MAV.

Finally, the SRR task has, over the past two years, developed an alternative form of rover state estimation for the accurate and reliable determination of rover position and orientation relative to a fixed reference frame. This technique uses an extended Kalman filter framework based on the work described in [3]. Within the SRR development, the registration of successive range maps generated by the rover's forward-looking hazard avoidance cameras are utilized to determine the frame-to-frame translation and rotation of the rover. This information is combined with dead reckoned estimates of the rover's translation and rotation to produce an optimized determination of the rover pose. This work is described in [7] and [2] and illustrated in Figure 12 for a 6+ m traverse within a soft-soil, rock-filled indoor sand pit.

5. FIDO ROVER TECHNOLOGIES

As described in Section 2, the 2003/05 MSR's Athena rover mission represents a significant increase in complexity over the recent Sojourner rover mission. The Athena rover carries seven science payload elements, including a multi-spectral imaging system, a microimager, a sample acquisition system, and four different spectrometers as compared to Sojourner's single science instrument, the Alpha Proton X-ray spectrometer. In addition, the Athena rover has over eight times the volume and six times the mass of the Sojourner rover. As such, the Athena rover represents a true sciencecraft and fulfills the need for a robotic field geologist on Mars.

To facilitate the successful operation of the Athena rover during the 2003/05 Mars Sample Return missions, a terrestrial prototype of the Athena rover is being used by the Athena science team for science and engineering testing associated with flight mission operations. The development of this robotic vehicle, known as FIDO (for Field Integrated, Design, and Operations) rover began in early 1998 with the conceptual design of the vehicle and culminated nine months later with the full-scale integration of the rover and its science payload [14]. In April 1999 (less than 14 months since the initial paper designs), the FIDO rover was successfully operated at the Silver Lake field test site outside Baker in California's Mojave desert. Figure 13 shows FIDO operating during this desert field test.

FIDO's mobility subsystem consists of a 6-wheel rocker-

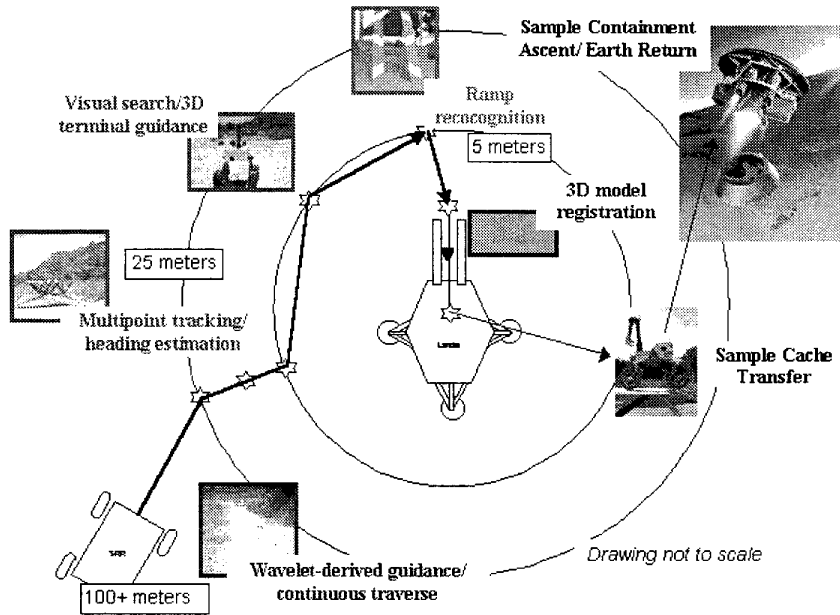


Figure 10. The operations scenario associated with the return to the lander.

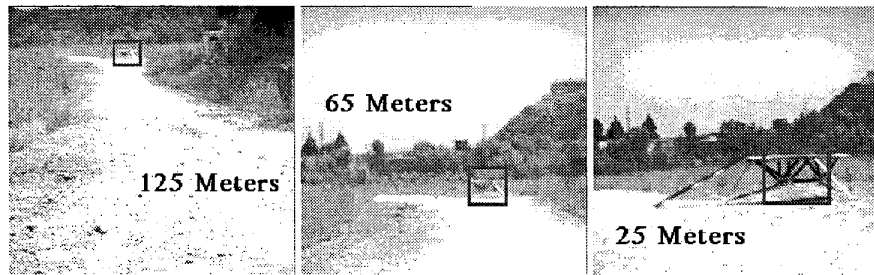


Figure 11. Wavelet-based lander detection and navigation.

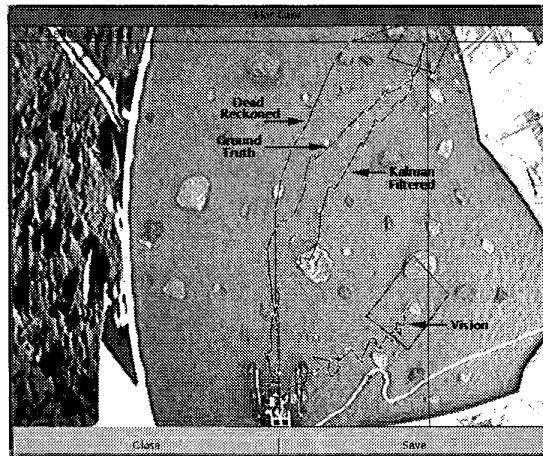
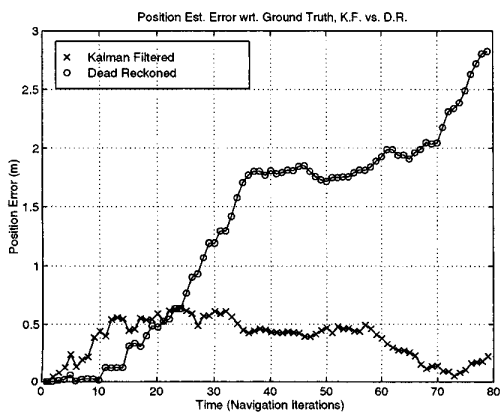


Figure 12. State estimation for rover pose determination.

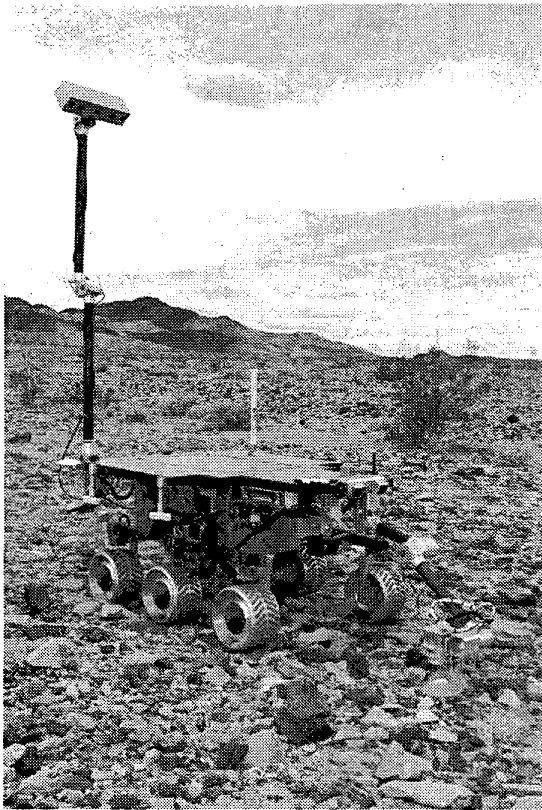


Figure 13. The FIDO rover during the Silver Lake field trial.

bogie suspension system that has been scaled up by a factor of 20/13 from the Sojourner design. This suspension system allows for the safe traverse over obstacles up to 30 cm in height. Each wheel is independently driven and steered using a Sojourner-derived actuation and encoder system. The top ground speed of the vehicle is 9 cm/sec. Approximate rover dimensions are 1 m in length, 0.8 m in width, 0.5 m in height, and 0.23 m ground clearance. The rover carries a four degrees-of-freedom deployable mast that stands 1.94 m off the ground surface at full extent. This mast provides the necessary pan-and-tilt control for panoramic imaging and point spectroscopy. FIDO also carries a four degrees-of-freedom instrument arm that is used to place the in situ suite of instruments on rock and soil targets.

The FIDO electronics are similar in nature to the SRR electronics with the CPU being a 80586 AMD processor running at a 133 MHz clock speed. The rover uses a PC104-based platform for all I/O functions, including a motion control system (D/A and encoder readers with closed-loop control in software) that can control up to 30 actuators simultaneously, two monochromatic and one color framegrabbers, digital I/O boards, A/D boards, low-pass filter and analog multiplexer boards, and a wireless Ethernet. Engineering sensors include front and rear stereo hazard avoidance camera systems, an inertial navigation system, and a sun sensor for absolute heading determination. A differential GPS unit is also integrated within the rover electronics for ground-truthing purposes only.

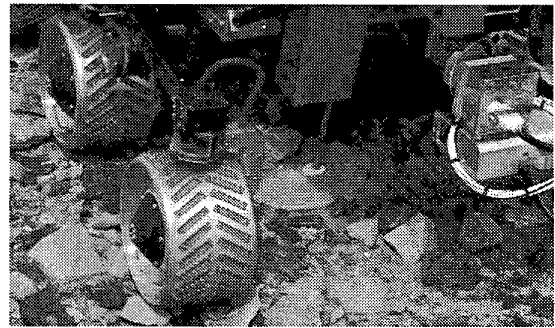


Figure 14. The miniature core drill acquiring a core sample from a carbonate rock at Silver Lake

The science payload on FIDO is analogous to the Athena payload. In particular, the remote sensing suite located on the FIDO mast includes a multi-spectral, narrow field-of-view *Pancam* stereo imaging system; a monochromatic, wider field-of-view *Navcam* stereo imaging system; and the optics for a near-IR point spectrometer that operates in the 1200 to 2500 nm wavelength region. The multi-spectral capability associated with the *Pancam* system is realized using a Liquid Crystal Tunable Filter (LCTF) that is tuned to the three near-IR wavelengths of 650, 750 and 850 nm. The in situ instrument suite attached to the end-effector of the FIDO instrument arm consists of a color microimager and a Moessbauer spectrometer that are used to determine the iron content of target rocks. A miniature core drill system, body-mounted to the rover, provides the capability to acquire and cache rock and soil samples. All of these instruments, with the exception of the near-IR point spectrometer (the flight mission uses a miniature thermal emission spectrometer in the mid-IR wavelength region), are breadboards of the Athena flight instruments.

In total, the science instrument and engineering sensing suites and the resulting FIDO rover system represent a terrestrial analog of the Athena rover that can be used to test and validate the Athena mission scenario and associated engineering functions. As such, the Athena science team led by Professor Steven Squyres, Athena PI, and Professor Raymond Arvidson, Athena Co-I, has worked with the FIDO engineering team since March 1999 to perform rover operations testing in support of the Athena rover mission. In particular, the desert field trial at the Silver Lake test site represented the first ever demonstration and validation of the sample acquisition phase of the Athena rover mission through the identification of target rocks, approach to the target rock, placement of the miniature core drill over the target rock, successful acquisition of a core sample using the miniature core drill, and return of these samples to a simulated landing site. Figure 14 shows the FIDO rover and associated core drill during the successful acquisition of a core sample from a carbonate rock. Future field trials in 2000 and 2001 will focus on flight-like rover operations, with the rover and science teams being sequestered at JPL while the rover is located at a remote test site. During such "blind" field trials, the full Athena mission scenario will be further validated, including sample acquisition and return to the lander as well as long-range science exploration and discovery.

6. SUMMARY

This paper has reviewed several recent research efforts that support upcoming MSR mission scenarios. Three research tasks, LRSR, SRR, and FIDO, have been developing and testing new capabilities in prototype rover platforms. LRSR research with Rocky 7 has developed four new techniques to enhance the functionality of autonomous long-range Mars rover navigation: intelligent sequencing, sensor constrained path planning, natural terrain visual localization, and Kalman Filter state estimation. SRR has developed a return-to-lander capability with visual tracking at various ranges, using techniques suitable to those ranges. It has also displayed visual odometry techniques. Finally, FIDO represents the culmination of the two core robotic technology programs since its development is based on the experiences gained within LRSR and SRR. As a result, it has become a standard integration and test system for the validation of rover navigation and control strategies.

7. ACKNOWLEDGMENTS

Large systems like these require the support of many people beyond the authors. We would like to recognize the following individuals for their invaluable contribution to the work described in this paper: the LRSR team includes J. (Bob) Balaram, Clark Olson, Sharon Laubach, Tara Estlin, Richard Petras, Darren Mutz, Greg Rabideau, and Mark Maimone; the SRR team includes Hrand Aghazarian, Terry Huntsberger, Yang Cheng, Mike Garrett, and Lee Magnone; the FIDO team includes Hrand Aghazarian, Terry Huntsberger, Anthony Lai, Randy Lindemann, Paul Backes, Brett Kennedy, Lisa Reid, Mike Garrett, and Lee Magnone.

The research described in this paper was carried out by the Jet Propulsion Laboratory, California Institute of Technology, under a contract with the National Aeronautics and Space Administration. Reference herein to any specific commercial product, process, or service by trade name, trademark, manufacturer, or otherwise, does not constitute or imply its endorsement by the United States Government or the Jet Propulsion Laboratory, California Institute of Technology.

REFERENCES

- [1] J. Balaram. Kinematic State Estimation for a Mars Rover. *Robotica, Special Issue on Intelligent Autonomous Vehicles*, Accepted for publication, 1999.
- [2] E. T. Baumgartner, P. C. Leger, P. S. Schenker, and T. L. Huntsberger. Sensor Fused Navigation and Manipulation from a Planetary Rover. In *Sensor Fusion and Decentralized Control in Robotic Systems, SPIE Proceedings 3523*, Boston, November, 1998.
- [3] E. T. Baumgartner and S. B. Skaar. An Autonomous Vision-Based Mobile Robot. *IEEE Transactions on Automatic Control*, 39(3):493–502, March 1994.
- [4] J-K. Chang and T. L. Huntsberger. Dynamic Motion Analysis using Wavelet Flow Surface Images. *Pattern Recognition Letters*, 20(4):383–393, 1999.
- [5] S. Chien, R. Knight, R. Sherwood, and G. Rabideau. Integrated Planning and Execution for Autonomous Spacecraft. In *IEEE Aerospace Conference*, Aspen CO, March 1999.
- [6] T. Estlin, G. Rabideau, D. Mutz, and S. Chien. Using Continuous Planning Techniques to Coordinate Multiple Rovers. In *IJCAI Workshop on Scheduling and Planning*, Stockholm, Sweden, August 1999.
- [7] B. D. Hoffman, E. T. Baumgartner, T. L. Huntsberger, and P. S. Schenker. Improved Rover State Estimation in Challenging Terrain. *Autonomous Robots*, 6(2), 1999.
- [8] S. Laubach. *Theory and Experiments in Autonomous Sensor-Based Motion Planning with Applications for Flight Planetary Microrovers*. PhD thesis, California Institute of Technology, May 1999.
- [9] S. Laubach and J. Burdick. An Autonomous Sensor-Based Path-Planner for Planetary Microrovers. In *IEEE International Conference on Robotics and Automation*, Detroit MI, 1999.
- [10] J. Matijevic et al. Characterization of the Martian Surface Deposits by the Mars Pathfinder Rover, Sojourner. *Science*, 278:1765–1768, December 5 1997.
- [11] C. Olson. Subpixel Localization and Uncertainty Estimation Using Occupancy Grids. In *IEEE International Conference on Robotics and Automation*, pages 1987–1992, Detroit, Michigan, May 1999.
- [12] C. Olson and L. Matthies. Maximum-likelihood Rover Localization by Matching Range Maps. In *IEEE International Conference on Robotics and Automation*, pages 272–277, Leuven, Belgium, May 1998.
- [13] P. S. Schenker et al. New Planetary Rovers for Long Range Mars Science and Sample Return. In *Intelligent Robots and Computer Vision XVII, SPIE Proceedings 3522*, Boston, November, 1998.
- [14] P. S. Schenker et al. FIDO Rover and Long-Range Autonomous Mars Science. In *Intelligent Robots and Computer Vision XVIII, SPIE Proceedings 3837*, Boston, September, 1999.
- [15] R. Volpe. Navigation Results from Desert Field Tests of the Rocky 7 Mars Rover Prototype. *International Journal of Robotics Research*, 18(7), 1999.
- [16] R. Volpe et al. Rocky 7: A Next Generation Mars Rover Prototype. *Journal of Advanced Robotics*, 11(4):341–358, 1997.